

Time scale of magma differentiation in arcs from protactinium-radium isotopic data

Yemane Asmerom } Department of Earth and Planetary Sciences, University of New Mexico, Albuquerque, New Mexico
S. Andrew DuFrane } 87131, USA
Samuel B. Mukasa } Department of Geological Sciences, University of Michigan, Ann Arbor, Michigan 48109, USA
Hai Cheng } Department of Geology and Geophysics, University of Minnesota, Minneapolis, Minnesota 55455,
R. Lawrence Edwards } USA

ABSTRACT

Absolute chronology of magma differentiation processes has been a long-desired goal, given its importance in understanding magma chamber dynamics and its connection to a fundamental understanding of the style and frequency of volcanic eruptions. Broad estimates of the duration of magma differentiation and overall crustal residence times have been made based on a variety of indirect approaches, such as physical models of magma chamber cooling, rates of crystal growth and settling, and long-lived radiogenic isotopes. In contrast, combined ^{231}Pa - ^{235}U data may provide a robust measure of the time scale of magma differentiation. Based on ^{231}Pa - ^{235}U , ^{230}Th - ^{238}U and ^{226}Ra - ^{230}Th data from Taal volcano, Luzon Arc, Philippine Archipelago, we show that ^{231}Pa - ^{235}U data may provide a robust direct measure of the time scale of magma differentiation. A closed-system magma fractionation model gives a ^{231}Pa - ^{235}U differentiation time scale in the range of 30 k.y., while the ^{226}Ra - ^{230}Th time scale is considerably younger. The time scales are reconciled if we consider either fluid-mixing or magma-mixing models. The fluid-mixing model gives a time scale of differentiation similar to the ^{231}Pa - ^{235}U closed-system time scale and is supported by the ^{230}Th - ^{238}U data. The magma-mixing model gives a considerably longer time, in the range of 55 k.y. The combined observations support the robustness of the ^{231}Pa - ^{235}U chronology, indicating a differentiation time scale in the range of 30 k.y., although this time scale for other volcanoes may vary depending on size and thermal state of the magma chamber. The ^{226}Ra - ^{230}Th closed-system model ages, which yield much younger estimates for magma differentiation, are not likely to reflect time scales of magma differentiation.

Keywords: time scale, differentiation, ^{231}Pa , ^{226}Ra , magma, uranium series.

INTRODUCTION

The composition of most igneous rocks at the surface is the result of significant modification in crustal-level magma chambers of more primitive mantle melts. This process of differentiation is a fundamental step in generating more chemically evolved lavas. Robust estimation of the time scale of differentiation is important for understanding magma evolution and eruption dynamics of volcanic centers (Sparks, 2003). Previous approaches to constraining magma residence time at crustal chambers and time scale of magma differentiation have included physical methods, such as estimates of crystal growth and settling (e.g., Marsh, 1989; Martin and Nokes, 1988). Long-lived radiogenic isotopes such as Rb-Sr and U-Pb have also been used to estimate residence times of large differentiated systems (e.g., Halliday et al., 1989; Christensen and DePaolo, 1991; Wolff and Ramos, 2003).

Technical advances in the analysis of uranium-series (U-series) isotopes have made it possible to use these isotope systems to evaluate magma chamber processes. The eventual decay of the two major isotopes of U, ^{238}U and ^{235}U , to ^{206}Pb and ^{207}Pb , respectively, involves a number of short-lived inter-

mediate daughters. One branch involves the decay of ^{234}U (an intermediate daughter of the decay of ^{238}U) to ^{230}Th and the decay of ^{230}Th (half-life 75,690 yr; Cheng et al., 2000) to ^{226}Ra (half-life of 1600 yr). The second branch involves the decay of ^{235}U to ^{231}Pa (half-life of 32 k.y.). The change in the daughter-parent ratio, expressed as an activity (number of atoms times the decay constant) ratio, reflects either fractionation by some process or time since a given ratio was established. If any parent-daughter pairs are left undisturbed, then their activity ratio converges to and stays at unity (secular equilibrium) after about seven half-lives of the shorter-lived nuclide. All information is lost once the pair achieves secular equilibrium. The potential use of these nuclides for igneous processes was recognized very early in the discovery of radioactivity. Analytical difficulties had limited their applications until recently; e.g., it was not until 1994 that the first high-precision ($^{231}\text{Pa}/^{235}\text{U}$; activity ratio) data on igneous rocks were made and reported by Pickett and Murrell (1997). Our results reported here are the first to combine ($^{231}\text{Pa}/^{235}\text{U}$), ($^{226}\text{Ra}/^{230}\text{Th}$), and ($^{230}\text{Th}/^{238}\text{U}$) data for differentiated lavas.

The samples for this study come from Volcano Island, the active center within the Taal volcano caldera complex of the Luzon Arc, Philippine Archipelago. The composition of the lavas varies from tholeiitic basalt ($\text{SiO}_2 = 50.5$ wt%) to compositionally evolved rhyodacites ($\text{SiO}_2 \sim 64.4$ wt%). Bulk composition and trace element data (except for U-Th data) were reported by Miklius et al. (1991). The lavas have a very narrow range in $^{87}\text{Sr}/^{86}\text{Sr}$ and $^{143}\text{Nd}/^{144}\text{Nd}$ isotopic values: 0.70449–0.70459 and 0.51281–0.51285, respectively (Mukasa et al., 1994). Their Pb isotopic values are also very similar, although less coherent than the Sr and Nd isotopic values. For example, their $^{206}\text{Pb}/^{204}\text{Pb}$ values vary from 18.554 to 18.639 (Mukasa et al., 1994). Based on trace element data, the lavas used in this study were previously thought to be related to each other by simple crystal fractionation of a common parental magma (Miklius et al., 1991). The lavas are historical flows that erupted within the past 300 yr, thus minimizing errors that may result from uncertainties in eruption age.

RESULTS

Typical of arc lavas, the lavas exhibit ^{238}U over ^{230}Th enrichment ($^{230}\text{Th}/^{238}\text{U}$) (activity ratios) from 0.915 to 0.951 (Table 1; complete U-series data are available in the data Repository¹); the small variation is related to bulk composition and is consistent with time-induced variation. The lavas also show ^{231}Pa over ^{235}U and ^{226}Ra over ^{230}Th enrichments, ($^{231}\text{Pa}/^{235}\text{U}$) 1.31–1.51, and ($^{226}\text{Ra}/^{230}\text{Th}$) 1.02–1.61 (Table 1; Figs. 1A, 1B). The 1968 basalt flow, MB-5, has the highest ^{231}Pa and ^{226}Ra enrichments, 1.31 and 1.61, respectively. There is general agreement that ^{231}Pa enrichment is generated in the mantle during melting (Asmerom et al., 2000; Bourdon et al., 1998; Thomas et al., 2002). Although there is no general consensus on the timing of ^{226}Ra enrichment, the large ^{226}Ra enrichments exhibited by arc lavas are attributed to fluid addition occurring in the mantle (Turner et al., 2001).

¹GSA Data Repository item 2005120, Table DR1, complete data and methods, and Appendix 1, complete descriptions on models and parameters, is available online at www.geosociety.org/pubs/ft2005.htm, or on request from editing@geosociety.org or Documents Secretary, GSA, P.O. Box 9140, Boulder, CO 80301-9140, USA.

TABLE 1. PROTACTINIUM, RADIUM, THORIUM, AND URANIUM DATA

	MgO	$(^{231}\text{Pa}/^{235}\text{U})^*$	$(^{226}\text{Ra}/^{230}\text{Th})_i^\dagger$	$(^{230}\text{Th}/^{238}\text{U})$
MB-5 Phil	7.29	1.506 ± 14	1.63 ± 5	0.917 ± 8
CY-3	6.02	1.464 ± 39	1.34 ± 6	0.936 ± 11
B-4	5.95	1.451 ± 14	1.34 ± 6	0.945 ± 8
CAL-1	5.65	1.435 ± 29	1.29 ± 6	0.924 ± 21
BAL-1-1			1.19 ± 5	
BAL-1-2			1.19 ± 4	
BAL-1-D			1.15 ± 5	
BAL-1 Average	1.97	1.312 ± 11	1.18 ± 6	0.941 ± 6
BM-8-1			1.13 ± 4	
BM-8-D			1.12 ± 4	
BM-8 Average	1.50	1.282 ± 25	1.13 ± 3	0.951 ± 12
TML-1			1.00 ± 19	
TML-2			0.995 ± 35	
TML-3D			0.989 ± 21	
TML-4D			1.006 ± 18	
Average			1.000 ± 10	

Note: See footnote 1 in text for complete data table and description of methods.

*Activity ratios and 2σ errors; activity is equal to the number of atoms multiplied by the decay constant for that nuclide.

†Initial activity ratios; uncertainties in initial ratios (values at time of eruption) reflect uncertainties in age estimates, 0.250 ka, and analytical uncertainty, except for the 1968 eruption (MB-5). For historical lavas initial corrections for U, Pa, and Th are insignificant. Values for the secular equilibrium standard and for Table Mountain Latite (TML) are measured values.

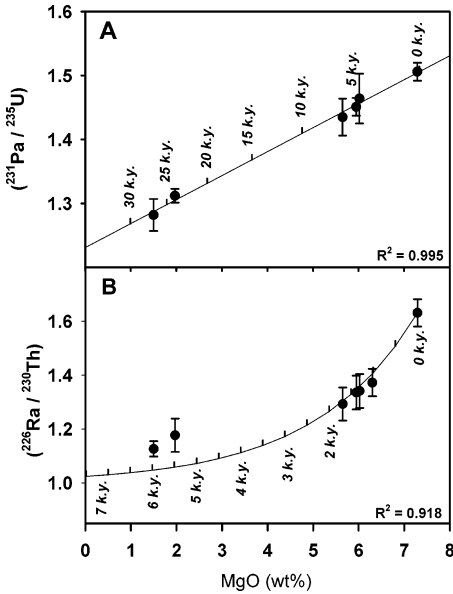


Figure 1. A: Variation of $(^{231}\text{Pa}/^{235}\text{U})$ vs. MgO of Taal lavas, ranging in composition from tholeiitic basalt (highest MgO) to evolved rhyodacite (lowest MgO). Samples fall on model isochron of magma differentiation. Age model relates degree of differentiation, expressed in MgO wt% values, to time scale of magma differentiation, using functional relationship derived from regression of MgO and $(^{231}\text{Pa}/^{235}\text{U})$ ($R^2 = 0.995$), assuming that each lava started from a separate batch of parental magma that had an initial value similar to the least-differentiated sample. Based on this model, time for differentiation from a composition of least-differentiated to most-differentiated lavas is ~27 k.y. B: Variation of $(^{226}\text{Ra}/^{230}\text{Th})$ with MgO (wt%) of samples shown in A. Data fall on a $(^{226}\text{Ra}/^{230}\text{Th})$ -MgO model age, constructed similarly to above model, but show more scatter than data in A. More important, differentiation ages are consistently younger than those derived from $(^{231}\text{Pa}/^{235}\text{U})$ data (<6 ka).

The salient feature of our Pa and Ra data is that the enrichments correlate with MgO content, an index of magma differentiation, with wt% MgO – $(^{231}\text{Pa}/^{235}\text{U})$ R^2 value of 0.995 (Fig. 1A). If these lavas had crystallized from the same parental magma (Miklius et al., 1991), there would be no variation in their $(^{231}\text{Pa}/^{235}\text{U})$ and $(^{226}\text{Ra}/^{230}\text{Th})$. It is more likely that they differentiated from different batches of magma that were similar in composition, and that variations in $(^{231}\text{Pa}/^{235}\text{U})$ and $(^{226}\text{Ra}/^{230}\text{Th})$ reflect the time scale of magma differentiation.

DISCUSSION AND CONCLUSIONS

In Figure 1A, we show results of a differentiation age model. If each of the lavas started from a distinct batch of magma that had a $(^{231}\text{Pa}/^{235}\text{U})$ value similar to the least-differentiated sample (basalt), their position on the curve shows the time of differentiation from the parent magma. Similarly, the MgO- $(^{226}\text{Ra}/^{230}\text{Th})$ variations are shown in Figure 1B, including results from an age model starting from the $(^{226}\text{Ra}/^{230}\text{Th})$ of the least-differentiated sample. The $(^{231}\text{Pa}/^{235}\text{U})$ chronology shows that differentiation from basaltic composition to the most evolved end member took 27 k.y. (Fig. 1A). In contrast, significantly shorter durations are implied by $(^{226}\text{Ra}/^{230}\text{Th})$ data. If the two chronometers were concordant, based on the $(^{231}\text{Pa}/^{235}\text{U})$ chronology, the most differentiated and second-most differentiated sample would have secular equilibrium $(^{226}\text{Ra}/^{230}\text{Th})$ values. Yet the most differentiated sample (BAL-8) has a slight measured ^{226}Ra excess outside of its 2σ error range, $(^{226}\text{Ra}/^{230}\text{Th})$ 1.025 ± 16 , which, when age corrected to the time of eruption, corresponds to an initial $(^{226}\text{Ra}/^{230}\text{Th})$ of 1.13 ± 3 . The second-most differentiated sample shows measurable enrichment, $(^{226}\text{Ra}/^{230}\text{Th}) = 1.071 \pm 43$, 2σ, with an initial ratio of 1.18

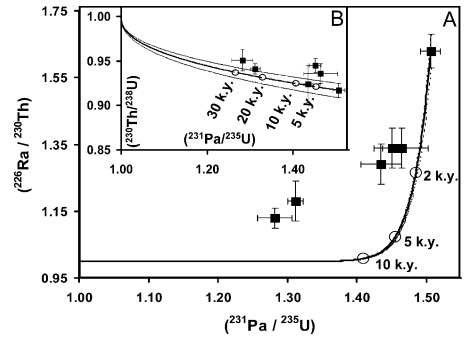


Figure 2. A: Pa-Ra concordia diagram, constructed using $(^{231}\text{Pa}/^{235}\text{U})$ and $(^{226}\text{Ra}/^{230}\text{Th})$ of least-differentiated samples as initial values and solving for activities of both systems at any given time. Samples with concordant $^{231}\text{Pa}-^{235}\text{U}$ and $^{226}\text{Ra}-^{230}\text{Th}$ ages should fall on concordia line; samples with $^{231}\text{Pa}-^{235}\text{U}$ ages greater than $^{226}\text{Ra}-^{230}\text{Th}$ ages fall to left of line. Our samples, except for one sample, fall far off concordia envelope, encompassing 2σ uncertainty of initial value. B: Pa-Th concordia diagram, constructed using similar approach to A. Note that in this case, all samples, except for one sample, fall within concordia envelope. Marked contrast between Pa-Ra and Pa-Th systematics suggests that Ra is likely nuclide that is mobile.

± 6. The $(^{231}\text{Pa}/^{235}\text{U})$ differentiation chronology for the intermediate composition sample ranges from 5 to 7 k.y. (Fig. 1A), while the $(^{226}\text{Ra}/^{230}\text{Th})$ chronology varies from 1 to <2.0 k.y. (Fig. 1B).

Given the coupling of the two uranium decay series, the Pa and Ra may be combined to construct a $(^{231}\text{Pa}/^{235}\text{U})$ - $(^{226}\text{Ra}/^{230}\text{Th})$ concordia diagram (Fig. 2A), allowing for the graphical analysis of the two chronologies. A similar diagram can also be constructed for the $(^{231}\text{Pa}/^{235}\text{U})$ - $(^{230}\text{Th}/^{238}\text{U})$ system (Fig. 2B). Concordant samples should fall on the solid lines in each diagram. All of our samples fall off the line on the $(^{231}\text{Pa}/^{235}\text{U})$ - $(^{226}\text{Ra}/^{230}\text{Th})$ diagram, except for one sample that is within 2σ analytical error. The most primitive lava by definition has to be on the concordia line. In contrast, all the samples except one fall on the $(^{230}\text{Th}/^{238}\text{U})$ - $(^{231}\text{Pa}/^{235}\text{U})$ concordia line, within analytical error. The broad concordance between the Pa-U and Th-U data and the lack of concordance between the Pa-U and Ra-Th data show that other processes likely affect Ra during differentiation. Although there are few samples with combined Pa and Ra data, no one has ever reported concordant Pa and Ra chronologies.

Here, two alternative models are considered to explain the discrepancy between the ^{231}Pa and ^{226}Ra chronologies. Model I is a magma replenishment model, based on the formulations of Hughes and Hawkesworth (1999). In this model, fresh magma with initial composition of the parent magma is added in an amount equal to the fraction of magma that

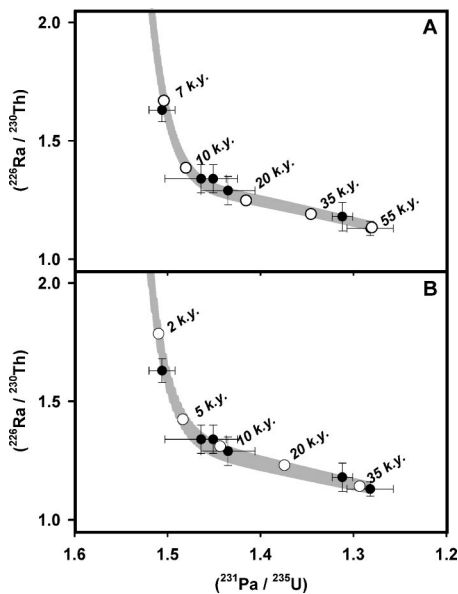


Figure 3. A: Results from magma replenishment model (Model I), shown as gray line. Data fit model well. Initial $(^{226}\text{Ra}/^{230}\text{Th})$ for magma and melt that is subsequently added is 10. This value is much higher than anything reported; Philippine lavas, even basalts, have low $(^{226}\text{Ra}/^{230}\text{Th})$ (e.g., BM-5). Figure is truncated to show portion relevant to data. Time scale of differentiation of ~50 k.y., from basalt to most evolved sample, is inferred. See text and Appendix 1 (see footnote 1) for detail on model. **B:** Results from fluid replenishment model (Model II), shown as gray line. Data fit model well. Differentiation time scales calculated from this model (from basalt with highest value to most differentiated sample) are similar to those obtained from $^{231}\text{Pa}/^{235}\text{U}$ chronology (Fig. 1A) and $^{230}\text{Th}/^{238}\text{U}$ chronology (Fig. 2B). See text and Appendix 1 (see footnote 1) for details on model.

crystallizes out, until the initial magma is completely replaced (F, degree of crystallization = 1). The model takes into account isotopic fractionation due to crystal fractionation and decay and magma mixing. Crystal fractionation and decay are implemented in alternating small steps in order to approximate a continuous process (Appendix 1 has details of parameters and implementation; see footnote 1). Best-fitting parameters were identified iteratively. The model that best fits the data, Figure 3, has the following values: $(^{226}\text{Ra}/^{230}\text{Th})_{\text{Melt}} = 10$, $(^{231}\text{Pa}/^{235}\text{U})_{\text{Melt}} = 1.57$, degree of crystallization of 0.36% per batch, and replenishment frequency of 200 yr and a duration of crystallization of 56 k.y. As can be seen in Figure 3A, the model fits the data well, but it requires that the magma added has a $(^{226}\text{Ra}/^{230}\text{Th})$ of 10. The $(^{226}\text{Ra}/^{230}\text{Th})$ value in Philippine lavas, even of basalts, are very low, e.g., BM-5 (Table 1). A value of 10 is almost twice the value observed even in lavas with the highest reported $(^{226}\text{Ra}/^{230}\text{Th})$ values (Turner et al., 2000).

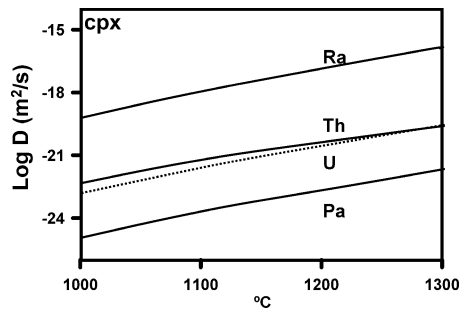


Figure 4. Diffusivities of Ra and Pa, calculated from elastic strain modeling, for clinopyroxene, based on Van Orman et al. (2001). Ra values are similar to those reported by Saal and Van Orman (2004). Diffusivities for U and Th are from Van Orman et al. (1998).

Model II is similar to Model I, except it assumes fluid rather than magma replenishment. Fluid replenishment is carried out exactly as in Model I, taking into account the effects of fractional crystallization, radioactive decay, and fluid addition on the $(^{226}\text{Ra}/^{230}\text{Th})$ and $(^{231}\text{Pa}/^{235}\text{U})$ values. The model best fits the data (Fig. 3B) with the following parameters: low concentration of Ra (1% of magma) but high $(^{226}\text{Ra}/^{230}\text{Th})$ of 70 and $(^{231}\text{Pa}/^{235}\text{U})$ of 1.528, degree of crystallization of 0.01% per replenishment cycle, replenishment frequency of 370 yr, and a duration of crystallization of 37 k.y. The fluid addition model has many attractive features. The time interval between the time of crystallization and the most differentiated sample is similar to that arrived at from the simple closed-system $(^{231}\text{Pa}/^{235}\text{U})$ model ages (Fig. 1A) and the ^{230}Th and ^{238}U chronology (Fig. 2B).

The apparent high $(^{226}\text{Ra}/^{230}\text{Th})$ required by the fluid addition model is justifiable on many grounds. Given the high diffusivity and fluid mobility of Ra (Cooper, 2001), it is unlikely that the Ra-Th will remain a closed system during the differentiation process in a fluid-dominated system such as an arc crustal magma chamber. In Figure 4 we show diffusivities for Ra and Pa calculated based on the elastic strain diffusion models described by Van Orman et al. (2001). The Ra values are similar to those reported by Saal and Van Orman (2004). We also show U and Th diffusivity data from Van Orman et al. (1998), all for diopside, which is the best characterized mantle mineral and is likely to be the principal carrier of U, Th, and radiogenic Ra (and Pa by extension). The diffusion data show that the Pa-Th system is the least vulnerable to diffusion re-equilibration. In contrast, the large difference between the diffusivities of Ra and U (almost 8 orders of magnitude, Fig. 4) and fluid solubility of Ra (an alkaline earth) should result in open-system behavior. Results from numerical calculation show that “a fluid trapped in isolated pockets at grain boundaries

due to incomplete wetting or percolating through lherzolite under steady conditions can achieve, and maintain during transport, $(^{226}\text{Ra}/^{230}\text{Th})$ in excess of 100 due to the preferential diffusion of ^{226}Ra out of clinopyroxene” (Feineman and DePaolo, 2003 p. 9).

Magma differentiation in arc magma chambers is likely to involve a large fluid fraction (Grove et al., 2002). To the extent that large ^{226}Ra enrichments in arc lavas, compared to intraplate and mid-ocean-ridge basalts, are attributed to fluid involvement in some fashion during melting (Turner et al., 2001), then fluid modification of $^{226}\text{Ra}/^{230}\text{Th}$ should be expected during magma differentiation. The eventual fate of the fluids involved during magma differentiation is not clear. One possibility is that magmatic fluids may be eventually lost as a vapor, leaving the melt enriched in fluid-mobile elements, such as Ra.

Although both the melt replenishment and fluid replenishment models take the effect of crystal fractionation into consideration, using bulk distribution coefficients for Pa, Ra, U, and Th, the potential effect of some important minerals, such as plagioclase with respect to Ra and accessory minerals with respect to U and Th, is difficult to assess. Ra is more compatible than U, Th, and likely Pa in plagioclase (Cooper, 2001; Cooper and Reid, 2003), and thus significant plagioclase fractionation could potentially deplete a given evolved melt with respect to Ra, as suggested by Zellmer et al. (2000). However, the effect on U-Th and U-Pa should be minimal; D_U and D_{Th} based on phenocryst data (Cooper and Reid, 2003) are low and of similar magnitude. Decrease in the Ba/Th ratios from ~55 (for the intermediate lavas) to 42 for the most differentiated lavas may indicate late-stage plagioclase removal. In contrast, the U/Th ratios of all the lavas are remarkably similar (0.28–0.29; Table 1), despite nearly a fourfold increase in concentration from basalt to the most differentiated lavas.

The global coherence in igneous rocks between $(^{230}\text{Th}/^{238}\text{U})$ and $(^{231}\text{Pa}/^{235}\text{U})$ and the apparent difficulty of reconciling the $(^{226}\text{Ra}/^{230}\text{Th})$ has been suggested as evidence for selective ^{226}Ra mobilization (Saal and Van Orman, 2004). Our results showing the lack of coherence between the $^{231}\text{Pa}/^{235}\text{U}$ and $^{226}\text{Ra}/^{230}\text{Th}$ chronologies (Figs. 1A, 1B, and 2A) and the coherence between $^{231}\text{Pa}/^{235}\text{U}$ and $^{230}\text{Th}/^{238}\text{U}$ chronologies (Fig. 2B) are in line with the global observations. Although we are not as pessimistic about the global igneous ^{226}Ra data, the numerical data reinforce our conclusions concerning the open-system nature of the ^{226}Ra chronology.

Although we think that the Ra data do not provide the full time scale of differentiation, they could provide a very useful constraint for postdifferentiation magma chamber residence time. In addition, as pointed out by Turner et

al. (2001), the large ^{226}Ra enrichments seen in primitive lavas may provide a constraint on the time scale of fluid-induced mantle melting and melt transfer, although even this aspect has been questioned (Feineman and DePaolo, 2003; Saal and Van Orman, 2004). The only other Ra-Pa study of lavas from a single volcanic center was reported by Vigier et al. (1999), although all the lavas were basalts. The lavas have similar ($^{231}\text{Pa}/^{235}\text{U}$), 2.19 ± 3 , 2.27 ± 7 , and 2.20 ± 2 , while the ($^{226}\text{Ra}/^{230}\text{Th}$) ranged from 1.866 to 1.302. Differences in ($^{226}\text{Ra}/^{230}\text{Th}$) model ages of these fluid-poor, minimally differentiated lavas may reflect differences in residence times, one of the possibilities suggested by Vigier et al. (1999).

Magma residence time scales obtained using long-lived radiogenic isotopes (e.g., Halliday et al., 1989; Christensen and DePaolo, 1991; Wolff and Ramos, 2003) tend to be too long and would preclude the existence of any ^{226}Ra , and in some cases ^{231}Pa , excesses. Long-lived radiogenic isotope values of differentiated lavas likely reflect relics of open-system magma behavior with respect to highly mobile alkaline earth elements like Sr (Wolff and Ramos, 2003). In this regard the Sr isotope data are indicative of the diffusive resetting of alkaline earth elements in general, including Ra. The short time scale calculated from our data may in part reflect size and thermal state of a magma chamber. Time scales of magma differentiation for larger volcanic systems should be somewhat longer, given their shallower thermal gradients. In addition, overall magma residence time could be higher than the time for simple magma differentiation. Long residence time inferred from U-Th isotopic data on zircons from large silicic volcanic centers (Reid et al., 1997; Vazquez and Reid, 2002) likely reflects overall magma residence time.

Given the ability to constrain the time scale of magma differentiation, it should in the future be possible to reassess processes related to magma chamber dynamics, such as recharge rates, which are crucial in building predictive capabilities.

ACKNOWLEDGMENTS

We thank Chris Hawkesworth and anonymous reviewers for very thoughtful and constructive reviews that improved the manuscript. Hawkesworth, through correspondence with Asmerom, shared generously his ideas and constructive suggestions. The work was supported by National Science Foundation grants EAR-0208095 and EAR-9980545 to Asmerom and EAR-0207830 to Mukasa. We benefited from discussions with Jim Van Orman and Mark Reagan.

REFERENCES CITED

Asmerom, Y., Cheng, H., Thomas, R., Hirschmann, M., and Edwards, R.L., 2000, Melting of the Earth's lithospheric mantle inferred from protactinium-thorium-uranium isotopic data: Na-

ture, v. 406, p. 293–296, doi: 10.1038/35018550.

Bourdon, B., Joron, J.-L., Claude-Ivanaj, C., and Allegre, C.J., 1998, U-Th-Pa-Ra systematics for the Grande Comore volcanics; melting processes in an upwelling plume: Earth and Planetary Science Letters, v. 164, p. 119–133.

Cheng, H., Edwards, R.L., Hoff, J., Gallup, C.D., Richards, D.A., and Asmerom, Y., 2000, The half-lives of uranium-234 and thorium-230: Chemical Geology, v. 169, p. 17–33, doi: 10.1016/S0009-2541(99)00157-6.

Christensen, J.N., and DePaolo, D.J., 1991, Time-scales of large volume silicic magma systems: Constraints from Sr isotopic systematics of phenocrysts and glass, Bishop Tuff, Long Valley, California: Geological Society of America Abstracts with Programs, v. 23, no. 5, p. A396.

Cooper, K.M., 2001, Time scales of magma generation, differentiation, and storage: Constraints from uranium-238–thorium-230–radium-226 disequilibria [Ph.D. thesis]: Los Angeles, University of California, 222 p.

Cooper, K.M., and Reid, M.R., 2003, Re-examination of crystal ages in recent Mount St. Helens lavas: Implications for magma reservoir processes: Earth and Planetary Science Letters, v. 213, p. 149–167, doi: 10.1016/S0012-821X(03)00262-0.

Feineman, M.D., and DePaolo, D.J., 2003, Steady-state $^{226}\text{Ra}/^{230}\text{Th}$ disequilibrium in mantle minerals: Implications for melt transport rates in island arcs: Earth and Planetary Science Letters, v. 215, p. 339–355, doi: 10.1016/S0012-821X(03)00454-0.

Grove, T.L., Parman, S.W., Bowring, S.A., Price, R.C., and Baker, M.B., 2002, The role of an H_2O -rich fluid component in the generation of primitive basaltic andesites and andesites from the Mt. Shasta region, N. California: Contributions to Mineralogy and Petrology, v. 142, p. 375–396.

Halliday, A.N., Mahood, G.A., Holden, P., Metz, J.M., Dempster, T.J., and Davidson, J.P., 1989, Evidence for long residence times of rhyolitic magma in the Long Valley magmatic system; the isotopic record in precaldra lavas of Glass Mountain: Earth and Planetary Science Letters, v. 94, p. 274–290, doi: 10.1016/0012-821X(89)90146-5.

Hughes, R.D., and Hawkesworth, C.J., 1999, The effects of magma replenishment processes on ^{238}U - ^{230}Th disequilibrium: Geochimica et Cosmochimica Acta, v. 63, p. 4101–4110, doi: 10.1016/S0016-7037(99)00311-7.

Marsh, B.D., 1989, Magma chambers: Annual Review of Earth and Planetary Sciences, v. 17, p. 439–474, doi: 10.1146/annurev.earth.17.050189.002255.

Martin, D., and Nokes, R., 1988, Crystal settling in a vigorously convecting magma chamber: Nature, v. 332, p. 534–536, doi: 10.1038/332534a0.

Miklius, A., Flower, M.F.J., Huijismans, J.P.P., Mukasa, S.B., and Castillo, P.R., 1991, Geochemistry of lavas from Taal Volcano, southwestern Luzon, Philippines; evidence for multiple magma supply systems and mantle source heterogeneity: Journal of Petrology, v. 32, p. 593–627.

Mukasa, S.B., Flower, M.F.J., and Miklius, A., 1994, The Nd-, Sr- and Pb-isotopic character of lavas from Taal, Laguna de Bay and Arayat volcanoes, southwestern Luzon, Philippines; implications for arc magma petrogenesis, in Hayes, D.E., ed., Tectonophysics, Volume 235: Amsterdam, Elsevier, p. 205–221.

Pickett, D.A., and Murrell, M.T., 1997, Observations of $^{231}\text{Pa}/^{235}\text{U}$ disequilibria in volcanic rocks: Earth and Planetary Science Letters, v. 148, p. 259–271.

Reid, M.R., Coath, C.D., Harrison, T.M., and McKeegan, K.D., 1997, Prolonged residence times for the youngest rhyolites associated with Long Valley Caldera; ^{230}Th - ^{238}U ion microprobe dating of young zircons: Earth and Planetary Science Letters, v. 150, p. 27–39, doi: 10.1016/S0012-821X(97)00077-0.

Saal, A.E., and Van Orman, J.A., 2004, The ^{226}Ra enrichment in oceanic basalts: Evidence for melt-cumulate diffusive interaction processes within the oceanic lithosphere: Geochimica et Cosmochimica Acta, v. 68, p. Q02008, doi:10.1029/2003GC00062.

Sparks, R.S.J., 2003, Forecasting volcanic eruptions: Earth and Planetary Science Letters, v. 210, p. 1–15, doi: 10.1016/S0012-821X(03)00124-9.

Thomas, R.B., Hirschmann, M.M., Cheng, H., Reagan, M.K., and Edwards, R.L., 2002, ($^{231}\text{Pa}/^{235}\text{U}$)-($^{230}\text{Th}/^{238}\text{U}$) of young mafic volcanic rocks from Nicaragua and Costa Rica and the influence of flux melting on U-series systematics of arc lavas: Geochimica et Cosmochimica Acta, v. 66, p. 4287–4309.

Turner, S., Bourdon, B., Hawkesworth, C., and Evans, P., 2000, ^{226}Ra - ^{230}Th evidence for multiple dehydration events, rapid melt ascent and the time scales of differentiation beneath the Tonga-Kermadec island arc: Earth and Planetary Science Letters, v. 179, p. 581–593, doi: 10.1016/S0012-821X(00)00141-2.

Turner, S., Evans, P., and Hawkesworth, C.J., 2001, Ultrafast source-to-surface movement of melt at island arcs from ^{226}Ra - ^{230}Th systematics: Science, v. 292, p. 1363–1366.

Van Orman, J.A., Grove, T.L., and Shimizu, N., 1998, Uranium and thorium diffusion in diopside: Earth and Planetary Science Letters, v. 160, p. 505–519, doi: 10.1016/S0012-821X(98)00107-1.

Van Orman, J.A., Grove, T.L., and Shimizu, N., 2001, Rare earth element diffusion in diopside; influence of temperature, pressure, and ionic radius, and an elastic model for diffusion in silicates: Contributions to Mineralogy and Petrology, v. 141, p. 687–703.

Vazquez, J.A., and Reid, M.R., 2002, Time scales of magma storage and differentiation of voluminous high-silica rhyolites at Yellowstone Caldera, Wyoming: Contributions to Mineralogy and Petrology, v. 144, p. 274–285.

Vigier, N., Bourdon, B., Joron, J.L., and Allegre, C., 1999, U-decay series and trace element systematics in the 1978 eruption of Ardukooba, Asal rift: Timescale of magma crystallization: Earth and Planetary Science Letters, v. 174, p. 81–97, doi: 10.1016/S0012-821X(99)00256-3.

Wolff, J.A., and Ramos, F.C., 2003, Pb isotope variations among Bandelier Tuff feldspars; no evidence for a long-lived silicic magma chamber: Geology, v. 31, p. 533–536, doi: 10.1130/0091-7613(2003)0312.0.CO;2.

Zellmer, G., Turner, S., and Hawkesworth, C., 2000, Timescales of destructive plate margin magmatism; new insights from Santorini, Aegean volcanic arc: Earth and Planetary Science Letters, v. 174, p. 265–281, doi: 10.1016/S0012-821X(99)00266-6.

Manuscript received 18 February 2005
Revised manuscript received 25 March 2005
Manuscript accepted 29 March 2005

Printed in USA